Chemical Engineering Science 197 (2019) 345–356

Contents lists available at ScienceDirect

Chemical Engineering Science

journal homepage: www.elsevier.com/locate/ces

Mathematical modelling of surface tension of nanoparticles in electrolyte solutions

Saheed Olawale Olayiwola, Morteza Dejam *

Department of Petroleum Engineering, College of Engineering and Applied Science, University of Wyoming, 1000 E. University Avenue, Laramie, WY 82071-2000, USA

HIGHLIGHTS

- Surface tension of nanoparticles (NPs) dispersed in deionized water is predicted.
- Effect of NPs size on surface tension of NPs dispersed in deionized water is studied.
- Change in surface tension of NPs dispersed in brine (electrolyte solution) is modeled.
- Dipole-dipole interaction, structural, and electric double layer effects are taken into consideration.

ARTICLE INFO

Article history:
Received 21 September 2018
Received in revised form 13 November 2018
Accepted 25 November 2018
Available online 2 December 2018

Keywords:
Nanoparticles
Surface tension
Electrolytes
Dipole-dipole interaction
Structural effect

ABSTRACT

Nanoparticles (NPs) have been successfully applied to reservoirs for enhanced oil recovery and fines migration mitigation at laboratory scale. Despite the successful implementation at laboratory scale, it is rarely applied at field scale. One of the major reasons for the delay in implementation is the lack of an appropriate model to predict the fluid-particles behaviour in the reservoir. An accurate prediction of the surface tension of the fluid system is particularly important in field design and development in the petroleum sector.

The surface tension of NPs in deionized water increases with increase in concentration of NPs. This study exploits the Debye-Hückel constants to calculate the mean activity coefficients of NPs in solution combined with the equation proposed by Li and Lu (2001) for single electrolyte solutions to estimate the change in surface tension.

However, NPs behaviour in brine (electrolyte solution) is different from the behaviour of mixture of different electrolytes. In deionized water, the surface tension of the fluid increases with increase in the NPs concentration, but NPs in electrolyte solutions behave as surface active agent decreasing the surface tension with increase in NPs concentration. This work includes the dipole-dipole interaction and structural effects along with the equation developed by Borwankar and Wasan (1988) for surface excess adsorption. This surface excess adsorption is applied to Li and Lu's equation for mixed electrolyte solutions to estimate the change in surface tension.

This study is able to model the surface tension of NPs with or without electrolyte. Here, the molecular interaction of NPs in deionized water and electrolyte solutions is considered to predict the fluid-surface tension. The free energy at the interface is affected by the intermolecular interaction of the NPs. This intermolecular interaction includes electrical double layer, dipole-dipole interaction, and structural effects. The proposed model shows a good agreement with the experimental data from previous studies.

1. Introduction

Surface tension is a physical property of liquid at the interface with the force acting perpendicular to the surface. It is an important property in the manufacturing and processing of various materials in several fields like medicine, drug production, biochemistry, bioscience, and engineering. Nanoparticles (NPs) application is currently growing in the field of petroleum engineering. It is especially applied in the drilling and exploration, reservoir monitoring and management as well as enhanced oil recovery (EOR) (Olayiwola and Dejam, 2019).

NPs have the capability to alter the rheological and the fluid properties as well as the wettability alteration of the rock. This

* Corresponding author.
E-mail address: mdejam@uwyo.edu (M. Dejam).

https://doi.org/10.1016/j.ces.2018.11.047
0009-2509/

behaviour is attributed to the high surface area to volume ratio of the particles (Negin et al., 2016; Kamal et al., 2017). NPs also have a great potential to alter the optical, electrical, and magnetic properties of the rock and the fluid (Bera and Belhaj, 2016; Engeset, 2012). The electrical and magnetic properties of nanomaterials have made them to be great tools for development of nanosensors used in imaging and characterization of rock and fluid systems during exploration (Negin et al., 2016; Bera and Belhaj, 2016; Engeset, 2012). Rheological properties of NPs is applied in drilling fluids to control the fluid loss and swelling of shale during drilling (Bera and Belhaj, 2016). NPs application is not limited to the drilling and exploration. It has successfully been used to improve oil recovery at the laboratory scale during EOR (Negin et al., 2016; Kamal et al., 2017; Zargartalebi et al., 2014). Increasing oil recovery is attributed to the wettability alteration and interfacial tension reduction (Negin et al., 2016).

Numerous studies on the adsorption of surface-active agents at the fluid-solid interface have been presented in the past. Several models on electrolytes that can successfully predict the surface tension have been proposed. Different approaches used in modelling of surface tension can be categorized into three (Stairs, 1995; Horvath, 1985; McCabe and Galindo, 2010):

(i) Direct calculation of the total works of ions at the surface separation,
(ii) The use of Gibbs adsorption equation in conventional thermodynamics, and
(iii) Statistical-mechanical methods using the radial distribution approach.

Ariyama (1937) used Debye-Hückel theory with potential energy of ions to calculate the surface tension of electrolytes. Lorenz (1950) showed that the increment in the surface tension is due to the total ions present in the solution. Electrostatic repulsion of the ions in electrolyte solutions is used as a basis for estimation of surface tension (Onsager and Samaras, 1934). Onsager and Samaras's equation was extended to include the effect of ionic polarization (Stairs, 1995) to calculate the surface tension. Polarization causes local dielectric saturation around the ion resulting in ion-induced dipole interaction in the image potential. Li et al. (1999) used Pitzer osmotic coefficient combined with Gibbs equation to calculate the surface tension of concentrated single and mixed electrolyte solutions. Buff and Stillinger (1956) presented statistical mechanical formula to estimate the surface tension of solid-liquid interface. Markovich et al. (2015) included the effects of the ionic size, ionic strength, and ion-surface interaction on the surface tension using the self-consistent theory.

Addition of electrolyte to solution causes an increase in the surface tension. This is attributed to the expulsion of ions from the surface outermost layer due to ionic repulsion (Onsager and Samaras, 1934; Fawcett, 2004). Petersen and Saykally (2006) showed that the degree of ionic polarization depends on the distance from the surface. The highly polarized ions induce a dipole moment on the anions that lures the cations towards the interface resulting in minimum Gibbs free energy. Chen et al. (2017) coupled Gibbs dividing surface with statistical associating fluid theory (ion-based SAFT-2) to model the surface tension of aqueous solutions of electrolyte and mixed electrolyte solutions with associating fluid at different temperatures and concentrations. Solvation of ions affects the thermodynamic properties of the electrolytes. Ion-water interaction and ion-ion interaction influence the structure of the electrolyte solutions, which directly impacts the surface tension (Andreev et al., 2018; Hey et al., 1981; Weissenborn and Pugh, 1996). The surface tension of an electrolyte solution is related to the nucleation-crystal controlled growth by the mean ionic activity in a saturated solution (solubility) (Christoffersen et al., 1991). Randles (1977) measured the contribution of each ion hydration energy to the surface potential in order to determine the surface tension of the solution. The change in the orientation of the polar water molecules may affect the surface potential of the electrolyte solution as well as the surface tension (Jarvis and Scheiman, 1968).

Although, several studies have proposed different models with accurate prediction to estimate the surface tension of both dilute and concentrated electrolyte solutions, there is virtually no model to the best of our knowledge that can predict the surface tension of NPs in solutions. The effect of NPs on surface tension becomes imperative with introduction of NPs to petroleum field for EOR. It is believed that NPs can alter the wettability of the rock towards more water-wet only, thereby improving the oil recovery. NPs can not only alter the wettability of the rock but also can alter the surface tension of the fluid. It is noted that different experiments have been conducted to determine the effect of NPs on the surface tension in the reservoir especially with surfactant, but only few data are available on the effect of NPs on surface tension in brine.

Bhuiyan et al. (2015) showed that the surface tension of different size of NPs increases with increase in the concentration and the size of the NPs. Tanvir and Qiao (2012) and Harikrishnan et al. (2017) reported a similar behaviour for surface tension with increase in NPs concentration using polar and slightly polar solvents. The increase in the surface energy is attributed to the Van der Waals forces.

This study presents a model to describe the effect of NPs in deionized water and brine on the surface tension using the well-established equations for electrolyte and surfactant solutions. To model the surface tension of NPs in deionized water, the Debye-Hückel theory for estimation of the mean ionic activities is combined with the equation proposed by Li and Lu (2001) for single electrolyte solutions. However, the equation for mixed electrolyte solutions is not sufficient to model the surface tension of NPs in brine. This work considers the adsorption of NPs in brine by including the effects of dipole-dipole interaction (Stairs, 1995), the structure of particles in the film (Kralchevsky and Denkov, 1995), and the electric double-layer (Borwankar and Wasan, 1988). The considered adsorption is combined with the li and Lu's equation for mixed electrolyte solutions to calculate the surface tension. The model is verified with experimental data from previous studies. As the outline of the article, first, the theoretical model is developed. Thereafter, the model is validated using the experimental data from previous studies. The results and discussion are then presented, which are followed by the conclusions.

2. Theoretical model

The interfacial phase region of NPs solutions is a continuous phase similar to that of electrolyte solutions with varying properties. For a solution at equilibrium, Gibbs (1906) proposed the dividing surface to deal with the continuous variation in the phase properties. The dividing surface is a mathematical plane separating the homogeneous bulk phase from the interface.

Addition of non-electrolytes to solution reduces the surface tension by lowering the surface energy. However, NPs behave similarly to electrolytes by increasing the surface tension. Gibbs equation (Gibbs, 1906) for surface excess adsorption of one component is as follows:

$$\frac{d\sigma}{d\ln a} = -RT\Gamma \tag{1}$$

where σ is the surface tension, a is the activities of the ions, R is the gas constant, T is the temperature, and Γ is the surface excess (Gibbs) adsorption of the component.

The Gibbs adsorption equation is extended for an aqueous solution of several electrolyte components at constant temperature and pressure (Adamson and Gast, 1997) as below:

$$-d\sigma = \Gamma_w d\mu_w^\sigma + \sum_i \Gamma_i d\mu_i^\sigma \tag{2}$$

where the subscripts i and w are the number of electrolyte components and water, respectively, and μ is the chemical potential of each component.

2.1. NPs in deionized water

The behaviour of NPs in water is very complex compared to an electrolyte. NPs behave as monomer, dimer, or complex molecules in water (Cheng et al., 2002). Adamson and Gast (1997) explained that the adsorption of non-electrolytes is confined to the monolayer similar to chemisorption of gases. The presence of solid in solution stretches/compresses the surface region by changing the distance between atoms. This leads to change in the surface tension when particles are added to water. The Gibbs adsorption equation can be written for NPs as shown in Eq. (3):

$$-d\sigma = \Gamma_w d\mu_w^\sigma + \sum_i \Gamma_{NP} d\mu_{NP}^\sigma \tag{3}$$

The chemical potential can be expressed in terms of the activities of the ions for water and NPs, respectively, as follows:

$$\mu_w^\sigma = \mu_w^{\sigma 0} + RT\ln a_w \tag{4}$$

$$\mu_{NP}^\sigma = \mu_{NP}^{\sigma 0} + RT\ln a_{NP} \tag{5}$$

where $\mu_w^{\sigma 0}$ and $\mu_{NP}^{\sigma 0}$ are the standard chemical potentials of water and NPs, respectively.

The chemical potential of low concentration of NPs can be expressed in terms of activities in a similar way as electrolytes (Fawcett, 2004):

$$\mu_w^\sigma = RT\ln a_w \tag{6}$$

$$\mu_{NP}^\sigma = RT\ln a_{NP} \tag{7}$$

Substituting Eqs. (6) and (7) into Eq. (3) results in:

$$d\sigma = -RT(\Gamma_w d\ln a_w + \Gamma_{NP} d\ln a_{NP}) \tag{8}$$

Fawcett (2004) explains that Γ_w and Γ_{NP} can not be measured independently, but they can be measured in relative to each other. Therefore, Eq. (8) can be reduced to:

$$d\sigma = -RT\Gamma_{NP} d\ln a_{NP} \tag{9}$$

If it is assumed that Henry's law for a dilute solution is valid here, Eq. (9) can be presented as follows:

$$d\mu = RTd\ln c_{NP} \tag{10}$$

The surface excess (Gibbs) adsorption for NPs is thus expressed as:

$$\Gamma_{NP} = -\frac{1}{RT}\left(\frac{\partial\sigma}{\partial\ln c_{NP}}\right) \tag{11}$$

where c_{NP} is the concentration of NPs.

The adsorption of NPs on the surface of a solution can be found using the Langmuir gas-solid adsorption (Langmuir, 1918) as presented by Li and Lu (2001) for electrolytes. Therefore, the surface excess (Gibbs) adsorption at different concentrations of NPs can be presented as follows:

$$\Gamma_{NP} = \Gamma_{NP}^{w0}\frac{K_{NP}a_{NP}}{1 + K_{NP}a_{NP}} \tag{12}$$

where Γ_{NP}^{w0} and K_{NP} are the saturated surface excess adsorption of NPs and the adsorption equilibrium constant of NPs, respectively. Both parameters are obtained from the correlations for the surface tension of NPs solution and dissolution of NPs in water.

Integrating Eq. (9) from $a_{NP} = 0$ to $a_{NP} = a_{\max}$ results in:

$$\Delta\sigma = -RT\Gamma_{NP}^{w0}\ln\frac{1}{1 + K_{NP}a_{\max}} \tag{13}$$

The ionic activity of NPs is determined by using the Debye-Hückel approach along with the assumptions that the ions of NPs are spherical and they are in contact with each other or separated by the solvent. The work done by a mole of ions to acquire their charges relative to other charges contributing to the Gibbs energy is given as (Fawcett, 2004):

$$\ln a_{NP} = -\frac{1}{RT}\frac{N_L z_i e_0^2}{8\pi\varepsilon_0\varepsilon_s}\left(\frac{\kappa}{1 + \kappa d}\right) \tag{14}$$

where

$$I = \sum_i z_i^2 c_i \tag{15}$$

where N_L is the Avogadro number, z_i is the charge number, e_0 is the charge ion, ε_0 is the permittivity of the free space, ε_s is the relative permittivity, d is the distance between the centers of ions, κ^{-1} is the Debye length, I is the ionic strength, and c_i is the concentration of the ion in solution.

Eq. (14) can be rewritten in terms of Debye- Hückel constants A_{DH} and B_{DH} as follows (Fawcett, 2004):

$$\ln a_{NP} = -\frac{A_{DH} z_i^2 I^{1/2}}{1 + B_{DH} d I^{1/2}} \tag{16}$$

where

$$A_{DH} = \frac{N_L e_0^2 F}{8\pi}\left(\frac{2000}{(\varepsilon_0\varepsilon_s RT)^3}\right)^{1/2} \tag{17}$$

$$B_{DH} = F\left(\frac{2000}{\varepsilon_0\varepsilon_s RT}\right)^{1/2} \tag{18}$$

where F is the Faraday constant.

2.2. NPs in brine

The behaviour of NPs in deionized water is identical to electrolyte solutions and the surface tension increases with increase in concentration of NPs, but NPs behave differently when they are added to the electrolyte solution. The mixture of different electrolytes in solution results in an increase in surface tension of the system, while NPs in brine (electrolyte solution) behave like surface active agent (surfactant) by decreasing the surface tension. Surface tension of NPs increases with an increase in electrolyte concentration (Sulaiman et al., 2015).

Surface tension of NPs results from the molecular interaction at the solid-liquid interface with adjacent molecules in the bulk phase (Fowkes, 1964). The interactions are due to the metallic bonds, the hydrogen bonds, or the London dispersion forces depending on the chemical nature of the molecules and the fluctuation of the electronic dipoles. The surface (free) energy across the interface is the sum of energies due to the London dispersion forces, the hydrogen bonds, the dipole-dipole interactions, the dipole-induced interactions, the π-bonds, the donor-acceptor bonds, and the electrostatic interactions (Fowkes, 1968). The surface energy of the interface is the outcome of all the forces which can be written as follows:

$$W_A = W_A^d + W_A^h + W_A^p + W_A^i + W_A^\pi + W_A^{da} + W_A^e + W_A^{os} + \cdots \quad (19)$$

where W_A is the surface energy and the superscripts *d, h, p, i, π, da*, e, and *os* are the free energy due to the London dispersion forces, the hydrogen bonds, the dipole-dipole interactions, the dipole-induced interactions, the π-bonds, the donor-acceptor bonds, the electrostatic interactions, and the structural oscillatory interactions, respectively.

This work extends the method presented by Li and Lu (2001) for the mixed electrolyte solutions to NPs in brine by including the effects of the above-mentioned forces. Li and Lu's equation for mixed electrolyte solutions is as follows:

$$\Delta\sigma = RT\sum_i^n \Gamma_i^{w0} \ln\left(1 - \frac{K_i a_i}{1 + \sum_j K_j a_j}\right) \quad (20)$$

where i and j represent the components present in the solution and n is the number of components.

2.2.1. The total surface excess (Gibbs) adsorption of NPs in brine

Contrary to the surface excess adsorption of NPs in deionized water, which is negative, the adsorption of NPs in brine is more complicated. The charge-dipole, dipole-dipole, and dispersive (Van der Waals) interaction differentiate NPs from the hard spheres (Shevchenko et al., 2006). The effect of the molecular interaction force is more pronounced in NPs. In the presence of electrolytes, the dispersion forces between the ions of NPs are important on the potential energy and the structural oscillatory forces (or solvation forces) also come into play as well as the diffusion layer effects.

The major unknown parameter in Eq. (20) is the Γ_i of the components in the solution. Several approaches have been used in order to determine the surfactant adsorption. These approaches are classified as 2-D gas approach and 2-D solution approach (Lucassen-Reynders, 1976). Borwankar and Wasan, 1988 extended the 2-D solution approach for electrostatic and electrokinetic aspects by including the double layer effect. The model is successfully applied to several surfactants, but it is not sufficient to model NPs in brine (electrolyte solution). The dipole-dipole interaction of NPs molecule and the solvation energy play significant roles in the stability of the colloidal solution.

By considering a solution of NPs in a single electrolyte solution (MX) for a real system, the solvation energy enables the NPs to acquire the charges. The ions present in the solution are the ions of NPs, M^+, and X^-. The ions of NPs compete with the electrolyte ions present in the solution. The ions of NPs can be positive or negative with respect to the distribution of M^+ and X^- ions in the solution. The Γ_i for electrolyte (MX) is well defined in several studies (Borwankar and Wasan, 1988; Li et al., 1999; Li and Lu, 2001; Cheng et al., 2002; Drzymala and Lyklema, 2012).

The surface excess adsorption is the integral of the difference of concentration in the interface and the bulk with respect to the ion position (Petersen and Saykally, 2006). The surface excess adsorption of surfactant defined by Borwankar and Wasan (1988) can be extended to that of NPs by including the dipole-dipole interaction and solvation energy as follows:

$$\Gamma_{NP}^{w0} = \Gamma_{NP} + \lambda_{DF} + \lambda_P + \lambda_{SF} \quad (21)$$

where the subscripts *DF, P,* and *SF* account for the effects of the diffusion layer, dipole-dipole, and solvation forces, respectively.

Borwankar and Wasan (1988) expressed the λ_{DF} for positive and negative charges in double layer as follows:

$$\lambda_{DF+} = -2c\sqrt{\frac{\varepsilon_0\varepsilon_s RT}{2F^2 c}}\left[1 - \exp\left(\frac{-F\psi_0}{2RT}\right)\right] \quad (22)$$

and

$$\lambda_{DF-} = 2c\sqrt{\frac{\varepsilon_0\varepsilon_s RT}{2F^2 c}}\left[\exp\left(\frac{F\psi_0}{2RT}\right) - 1\right] \quad (23)$$

where c is the concentration of the ions in the bulk phase and ψ_0 is the potential of the ions.

In the double layer, the free charges on the surface, the unequal adsorption of ions of opposite charges, and the net orientation of dipoles are present that cause a drop in potential of the interface (Drelich, 2016). The dipole-dipole interaction is due to the difference in electronegativity between the electrolyte ions and the ions of NPs. NPs have the tendency to be organized into a variety of ordered shapes like chains, rings, and free-floating sheets (Tang et al., 2002; Cho et al., 2005; Tang et al., 2006). Entropy in addition to the dipole-dipole interaction plays a significant role especially in unstable colloidal (Bolhuis et al., 1997; Talapin et al., 2007).

Based on the kinetic principle, the concentration of solute particles at a distance of x from the surface boundary is a function of the work, $W(x)$, required to bring the ion to that position. The relationship is expressed by the Maxwell-Boltzmann equation as follows (Onsager and Samaras, 1934, Adamson and Gast, 1997):

$$c(x) = c(\infty)\exp(-W(x)/kT)) \quad (24)$$

where is k is the Boltzman constant, $W(x)$ is the potential energy at a distance x from the surface boundary, and $c(\infty)$ is the concentration in the bulk phase. Therefore, the general equation of surface excess adsorption is expressed as follows (Stairs, 1995; Onsager and Samaras, 1934):

$$\Gamma_i = c(\infty)\int_0^\infty [\exp(-W(x)/RT) - 1]dx \quad (25)$$

Consider a very small concentration of NPs in strong electrolyte solutions, the NPs and electrolyte ions are assumed to be hard spheres of the same radius of R_i at a distance r from each other. The positive ions are repelled from the surface while the negative ions are attracted. Consequently, the anions of the electrolyte and the NPs are present at the surface. The difference in electronegativity between the negative ion of electrolyte (X^-) and the ion of NPs, which induces the dipole-dipole interaction. The dipole moment of ion of NPs is μ_1 and the dipole moment of the electrolyte X^- ion is μ_2. Assuming the ions are moving randomly, the interaction energy due to the induced dipole-dipole interaction between two ions is defined by Keesom energy as follows (Adamson and Gast, 1997):

$$W(x) = -\frac{2}{3kT}\frac{\mu_1^2\mu_2^2}{(4\pi\varepsilon_0\varepsilon_s)^2 r^6} \quad (26)$$

The potential energy due to the dipole moment alters the surface tension. The change in surface tension is proportional to the surface excess adsorption from the dipole-dipole interaction.

The charge density due to ion at position x can be expressed as follows:

$$\rho_c = c(x)z_i F \quad (27)$$

The total charge density is the sum of the contributions from all the dipole-dipole interactions (Fawcett, 2004; Adamson and Gast, 1997):

$$\rho_c = \sum_i c(\infty)\, Fz_i \exp\left(-\frac{W(x)}{RT}\right) \quad (28)$$

where ρ_c is the (total) charge density.

The divergence of the gradient of the electrical potential at a given point can be related to the total charge density at that point through the Poisson's equation:

$$\nabla^2\psi = -\frac{\rho_c}{\varepsilon_0\varepsilon_s} \quad (29)$$

By substituting Eq. (28) into Eq. (29), the Poisson-Boltzmann equation can be obtained as follows:

$$\nabla^2\psi = -\frac{\sum_i z_i Fc(\infty)\exp\left(-\frac{W(x)}{RT}\right)}{\varepsilon_0\varepsilon_s} \tag{30}$$

The solution to Eq. (30) was presented (Gouy, 1910; Chapman, 1913; Debye and Hückel, 1923) and summarized in previous studies (Kruyt, 1952; James and Parks, 1982). This solution is applicable to the dipole-dipole interaction as described below.

It is considered that the dipole-dipole interaction between the electrolyte ion and the NPs ion is acting perpendicular to each other at the interface along the one-dimensional (1-D) plane in the x-direction. Therefore, the Poisson-Boltzmann equation for diffuse layer becomes:

$$\frac{d^2\psi}{dx^2} = -\frac{\sum_i z_i Fc(\infty)\exp\left(-\frac{W(x)}{RT}\right)}{\varepsilon_0\varepsilon_s} \tag{31}$$

The field becomes zero when the distance between the ions exceeds the local field of the ions. The potential drop across the diffuse layer due to the dipole-dipole interaction can be expressed as follows:

$$\left(\frac{d\psi}{dx}\right)^2 = \frac{4RTc(\infty)}{\varepsilon_0\varepsilon_s}\left(\cos h\left(\frac{W(x)}{RT}\right) - 1\right) \tag{32}$$

For a simple 1-1 electrolyte and 1-1 NPs, Eq. (32) turns to:

$$\frac{d\psi}{dx} = -\sqrt{\frac{8RTc(\infty)}{\varepsilon_0\varepsilon_s}}\sinh\left(\frac{W(x)}{2RT}\right) \tag{33}$$

The surface excess adsorption resulting from the dipole-dipole interaction between the ions of electrolyte and NPsin the diffuse layer can be written as below (Fawcett, 2004):

$$\lambda_p = c(\infty)\int_0^\infty\left(\exp\left(\frac{W(x)}{RT}\right) - 1\right)dx \tag{34}$$

Using the expression in Eq. (33) for the field in diffuse layer, the surface excess adsorption due to the anions of the electrolyte and the NPs, Eq. (34), can be expressed as follows:

$$\lambda_p = -\frac{Fc(\infty)}{RT}\sqrt{\frac{8RTz_i c(\infty)}{\varepsilon_0\varepsilon_s}}\int_\psi^0(\exp(W(x)/2RT))d\psi \tag{35}$$

Consequently, the surface excess adsorption due to the dipole-dipole interaction, Eq. (35), can be expressed as below:

$$\lambda_p = -F\Gamma_i = Fc(\infty)\sqrt{\frac{\varepsilon_0\varepsilon_s}{8RTc(\infty)}}(1-\exp(W(x)/2RT)) \tag{36}$$

2.2.2. Solvent structure

The structural order of fluid molecules near the interface produces oscillatory forces, which are vital in determination of the thermodynamic properties of continuum media (Andreev et al., 2018; Adamson and Gast, 1997). The oscillatory forces can be referred to hydration or solvation forces as well. Pairs or group of ions having zero net charges possess hydration energy (Andreev et al., 2018; Randles, 1977). Andreev et al. (2018) explains that the ion-water dispersion has a direct impact on the surface tension. Kralchevsky and Denkov (1995) proposed a model for the oscillatory energy, which depends on the film thickness and the particle volume fraction. The latter is a function of the film thickness and the concentration of electrolyte (Nikolov et al., 1990).

The potential due to the structural forces from the particles is given by Kralchevsky and Denkov (1995) as follows:

$$W^{os}(h) = \begin{cases} F(h), & h \geqslant d \\ F(d) - P_0(d-h), & 0 \leqslant h \leqslant d \end{cases} \tag{37}$$

where

$$F(h) = \frac{P_0 d_1 \exp\left(\frac{d^3}{d_1^2 d_2} - \frac{h}{d_2}\right)}{4\pi^2 + (d_1/d_2)}\left[\frac{d_1}{d_2}\cos\left(\frac{2\pi h}{d_1}\right) - 2\pi\sin\left(\frac{2\pi h}{d_1}\right)\right] \tag{38}$$

$$P_0 = \rho kT\frac{1+\varphi+\varphi^2-\varphi^3}{(1-\varphi)^3} \tag{39}$$

$$\rho = \frac{6\varphi}{\pi d^3} \tag{40}$$

where φ is the particle volume fraction, ρ is the particle number density, d, d_1, and d_2 are the diameter of the particles, oscillatory period, and decay length of the particles under oscillatory force, respectively.

Hachisu et al. (1973) observed a structural order of particles at the interface for which the potential can not be described by the concept proposed by Onsager and Samaras. The structural order of particles occurs at a short range in the liquid (Fawcett, 2004). The concept of an electrical double layer is used to describe the interface separation between the phases. The same concept is applied by Wasan and Nikolov (2003) to NPs using the concept of interaction energy for structural forces proposed by Kralchevsky and Denkov (1995). Nikolov et al. (1989) explained the importance of the particle size in determination of the threshold concentration for the appearance of an ordered structure based on the theoretical findings from Van Megen and Snook (1976). At a small distance of separation, the oscillatory forces due to the granularity of the liquid is very important (Horn and Israelachvili, 1980).

Using Eq. (34) and substituting the $W(x)$ by the $W^{os}(h)$ give:

$$\lambda_{SF} = c(\infty)\int_h^\infty(\exp(-W^{os}(h)/kT)-1)dh \tag{41}$$

Eq. (41) can be converted to the following equation using the procedure in Appendix A (where the detailed derivation can be found):

$$\lambda_{SF} = c(\infty)\sqrt{\frac{\varepsilon_0\varepsilon_s}{8kT\rho_{ci}c(\infty)}}\left(1-\exp\left(-\frac{W^{os}(h)}{2kT}\right)\right) \tag{42}$$

The total surface excess adsorption of the mixture of NPs and electrolytes in Eq. (21) is substituted into Eq. (20) to estimate the surface tension. It is noted that the expressions for the terms in Eq. (21) are obtained using Eqs. (11), (22), (23), (36), and (42). The oscillatory period and the decay length of the particles are defined in Appendix B.

3. Model validation

The model is validated using the experimental data from the previous studies. Section 3.1 shows the validation for the surface tension of NPs in deionized water while Section 3.2 exhbits the validation for the surface tension of NPs in brine (electrolyte solution). Table 1 summarizes the list of parameters used in the proposed model.

3.1. NPs in deionized water

This study models the surface tension of air-water with dispersed NPs. The surface tension increases with increase in concentration of the NPs. Eq. (13) in combination with the Debye-Hückel constants is used to estimate the surface tension. The model is validated by using the experimental data from Bhuiyan et al. (2015)

Table 1
Parameters used in the proposed model.

Parameter	Values	Unit
N_L	6.02214×10^{23}	/mol
ρ_w	0.99705	g/cm^3
ε_0	80	Dimensionless
ε_s	8.85×10^{-12}	Farad/m
k	1.38×10^{-23}	J.mol/K
e_0	1.60×10^{-19}	C
R	8.3145	J/K

and Harikrishnan et al. (2017) for several NPs, including silica, Al_2O_3, and TiO_2. To understand the concept used in this work, each NPs is analyzed separately starting with silica, followed by alumina and TiO_2.

Silica can exist as both monomer and dimer and even as a complex form in true aqueous solution (O'Connor and Greenberg, 1958; Bassett, 1973; Rimstidt and Barnes, 1980). Several reaction mechanisms of silica in water were defined in previous studies (O'Connor and Greenberg, 1958; Alexander et al., 1954). The stable state of silica in water can be in different forms, which lead to variation in the adsorption equilibrium constant. The adsorption equilibrium constant is estimated from the kinetic reaction and the solubility of silica from literature (O'Connor and Greenberg, 1958; Alexander et al., 1954). However, the size of nanoparticles does not have an influence on the adsorption (Metin et al., 2012). Some of the reactions are listed here:

$$SiO_{2_{(qtz)}} + 2H_2O \rightleftarrows H_4SiO_{4_{(aq)}} \tag{43}$$

$$SiO_2(qtz) \underset{+H_2O}{\leftrightarrows} SiO_2(aq) \tag{44}$$

$$2SiO_{2_{(monomer)}} \rightleftarrows Si_2O_{4_{(dimer)}} \tag{45}$$

$$SiOSi_{(surf)} + H_2O \rightleftarrows SiOH_{(surf)} + SiOH_{(surf)} \tag{46}$$

$$SiOH_{(surf)} \rightleftarrows SiOSi_{(surf)} + H_2O_{(vap)} \tag{47}$$

The adsorption equilibrium constant, K, of silica used in this work is between 10^1 and 10^3 (Metin et al., 2012; Jiang et al., 2018, Bassett, 1973 Stillings and Brantley, 1995; Newton and Manning, 2003). The size of the NPs is assumed to be uniform, spherical, and the particles are in contact with each other. The distance between the centers of the ions of NPs is equivalent to the size or diameter of the particles. The surface (Gibbs) excess adsorption is calculated by using the average of obtained values from Eq. (11), which is equal to -1.06 $\times$ 10^{-7} mol/m^2. The calculated value here is the same as the one reported by Ferdous et al. (2012).

The blue and red circles in Fig. 1 represent the experimental data of surface tension for 5–10 nm and 10–20 nm size of silica NPs, respectively. The blue and red solid curves obtained from the proposed model in this study refer to the above-mentioned size of silica NPs. Other parameters used in the calculation of the surface tension are listed in Table 2. The reference surface tension of air-water without NPs used for the experiments conducted by Bhuiyan et al. (2015) is 69.11 mN/m at 25 °C. The results obtained using the proposed model are in good agreement with the experimental data.

The blue[1] and red circles in Fig. 2 represent the surface tension of the 13 nm and 50 nm size of alumina NPs, respectively, from the experiments conducted by Bhuiyan et al. (2015) at 25 °C while the green circles are the experimental data from Harikrishnan et al. (2017) with 20 nm size at temperature of 30 ± 2 °C. The blue, red, and green curves in this figure are the obtained results from the proposed model in this study corresponding to the above-noted size of alumina NPs. The reference values of surface tension for air-water without NPs used in the experiments conducted by Bhuiyan et al. (2015) and Harikrishnan et al. (2017) are 69.11 mN/m and 71.5 mN/m, respectively. Other parameters used in the calculation of the surface tension are listed in Table 3. The obtained results from the proposed model are in good agreement with the experimental data.

[1] For interpretation of color in Figs. 1–3, the reader is referred to the web version of this article.

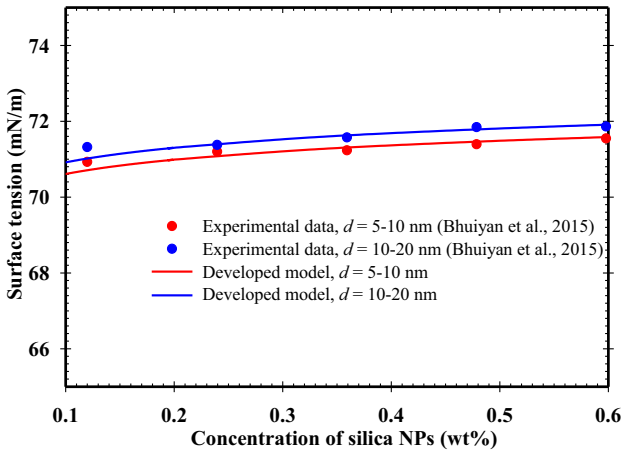

Fig. 1. Surface tension of dispersed silica NPs in deionized water versus concentration of silica NPs using the parameters listed in Tables 1 and 2. The results from the proposed model in this study are compared with the experimental data in literature (Bhuiyan et al., 2015).

Table 2
Parameters used for estimating the surface tension of silica NPs in deionized water.

Parameter	Values	Unit
ρ_{silica}	2.65	g/cm^3
K_{silica}	55	Dimensionless
T	25	°C
d	5–20	nm
MW	60.08	g/mol

The surface excess (Gibbs) adsorption of alumina used in the calculation of the surface tension is -1.2 $\times$ 10^{-7} mol/m^2, which is close to the one reported by Siracusa and Somasundaran (1987). Calculation of the adsorption equilibrium constant of alumina is as complicated as calculation of that of silica due to the complex reactions during the adsorption process of the water or hydrogen ions. Franke et al. (1987) and Lefevre et al. (2002) presented the reactions for the dissolution of alumina as follows:

Hydration:

$$Al_2O_{3_{(s)}} + 3H_2O_{(l)} \rightleftarrows 2Al(OH)_{3_{(s)}} \tag{48}$$

$$Al_2O_{3_{(s)}} + H_2O_{(l)} \rightleftarrows 2AlOOH_{(s)} \tag{49}$$

Hydrogen ion adsorption:

$$AlOOH_{(s)} + H^+_{(aq)} \rightleftarrows 2Al(OH)^+_{2_{(aq)}} \tag{50}$$

$$Al(OH)_{3_{(s)}} + H^+_{(aq)} \rightleftarrows Al(OH)^+_{2_{(aq)}} + H_2O_{(l)} \tag{51}$$

This shows that the composition of the alumina in deionized water can exist in different forms, which result in variation in the adsorption equilibrium constant.

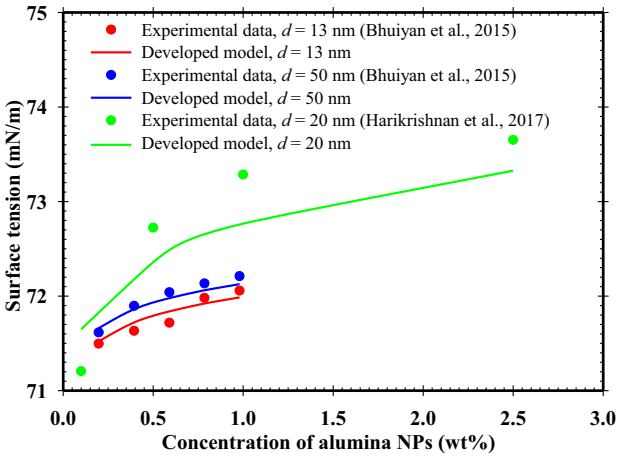

Fig. 2. Surface tension of dispersed alumina NPs in deionized water versus concentration of alumina NPs using the parameters listed in Tables 1 and 3. The experimental data used here were reported by Bhuiyan et al. (2015) and Harikrishnan et al. (2017).

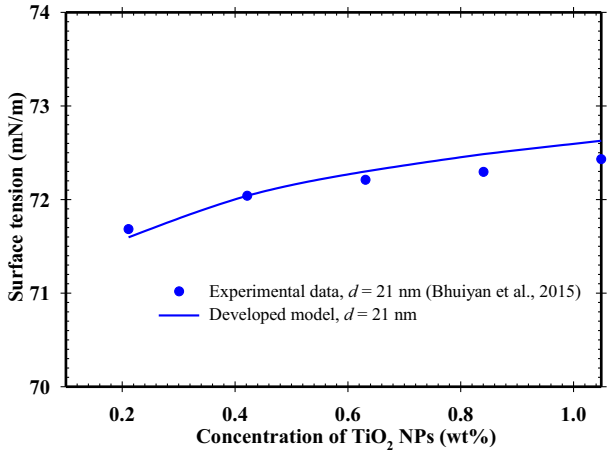

Fig. 3. Surface tension of dispersed TiO_2 NPs in deionized water versus concentration of TiO_2 NPs using the parameters listed in Tables 1 and 4. The results from the proposed model in this study are compared with the experimental data in literature (Bhuiyan et al., 2015).

Table 3
Parameters used for estimating the surface tension of alumina NPs in deionized water.

Parameter	Values	Unit
$\rho_{alumina}$	3.95	g/cm^3
$K_{alumina}$	10^3–10^4	Dimensionless
T	25–30	°C
d	13–50	nm
MW	102	g/mol

The reaction of all NPs in water is complex and TiO_2 is not an exception. Dissolution of TiO_2 in water produces several products, which may be in stable or unstable forms (Nowotny et al., 2010; Kobayashi et al., 2007). The adsorption equilibrium constant used here is estimated from the experimental data reported by Laysandra et al. (2017) as listed in Table 4. The surface excess (Gibbs) adsorption is estimated in a similar way to silica and alumina as -1.29 × 10^{-7} mol/m^2. The reactions for TiO_2 dissolution in aqueous solution is given as follows:

$$TiO_{2_{(s)}} + 2H_2O_{(l)} \rightleftarrows H_4TiO_{4_{(aq)}} \quad (52)$$

$$H^+_{(aq)} + TiO_{2_{(s)}} + e' \rightleftarrows TiO - OH_{(s)} \quad (53)$$

The blue circles in Fig. 3 represent the experimental data of surface tension for 21 nm size of TiO_2 NPs from the experiments conducted by Bhuiyan et al. (2015) while the blue curve shows the results obtained from the proposed model in this study. The reference surface tension of air-water without NPs used for the experiments conducted by Bhuiyan et al. (2015) is 69.11 mN/m. Other parameters used in the calculation of the surface tension are listed in Table 4. The results obtained from the proposed model are in good agreement with the experimental data.

Table 4
Parameters used for estimating the surface tension of TiO_2 NPs in deionized water.

Parameter	Values	Unit
ρ_{TiO2}	4.23	g/cm^3
K_{TiO2}	345	Dimensionless
T	25	°C
d	21	nm
MW	80	g/mol

3.2. NPs in brine

Interestingly, the surface tension of NPs dispersed in brine(electrolyte solution) decreases with increasing concentration of NPs. The results obtained from the proposed model in this study are validated using the experimental data reported by Sulaiman et al. (2015) and Zallaghi et al. (2018) for silica NPs dispersed in brine. The proposed model is not validated for other NPs due to lack of experimental data. The parameters used here to calculate the surface tension of dispersed silica NPs in brine are listed in Tables 1 and 5. Zallaghi et al. (2018) conducted experiments to measure the surface tension of dispersed NPs in brine at room temperature of 26 °C using hydrophilic silica NPs with an average diameter of 7 nm. The concentration of NaCl used during the experiments does not exceed 3 × 10^4 ppm (3 wt%) because the solution becomes unstable at 4 × 10^4 ppm (4 wt%) or larger concentrations of NaCl. The calculated values of surface tension from the proposed model in this study are validated using the experimental data reported by Zallaghi et al. (2018) as shown in Fig. 4. The proposed model is also compared and validated with the experimental data reported by Sulaiman et al. (2015) for the interfacial tension (IFT) of oil-water as shown in Fig. 5. The silica NPs used in the experiments have a size range of 20–30 nm and a density of 2.4 g/cm^3. The silica NPs were dispersed in five solutions with different concentrations of NaCl ranging from 0.3 to 4 wt%. The concentration of silica NPs dispersed in the solution ranges from 0.01 to 0.1 wt%. The results obtained from the proposed model in this study are validated using the experiment data reported by Sulaiman et al. (2015) as depicted in Fig. 5. The dipole-dipole moment used in the proposed model to calculate the surface excess adsorption resulting from the dipole-dipole interaction is reported by Müller and Woon (2013).

Table 5
Parameters used for solution of silica NPs and brine.

Parameter	Values	Unit
h	0–110	nm
φ	0–0.5	Dimensionless
d	3.5–30	nm
T	26	°C
μ_1	4.070	Debye
μ_2	3	Debye
r	1–100	nm

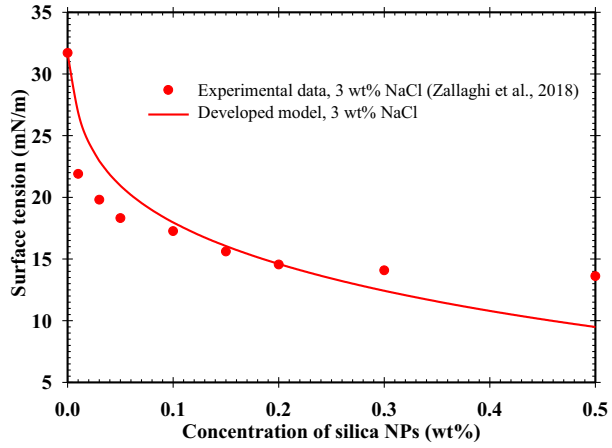

Fig. 4. Surface tension of silica NPs in 3 wt% NaCl solution using the parameters listed in Tables 1 and 5. The results from the proposed model in this study are compared with the experimental data in literature (Zallaghi et al., 2018).

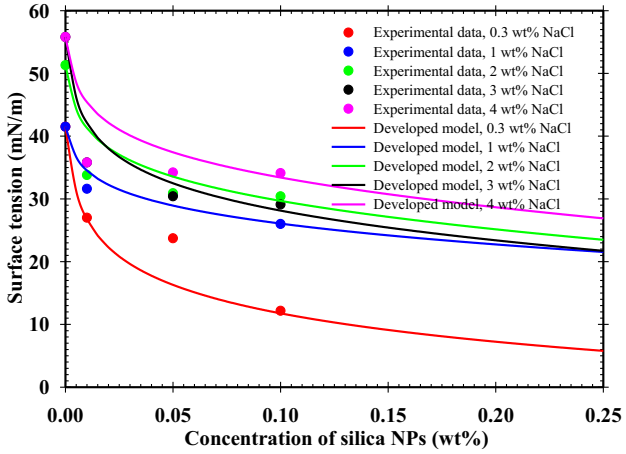

Fig. 5. Interfacial tension of oil-water modifies with different concentrations of NaCl and silica solution using the parameters listed in Tables 1 and 5. The results from the proposed model in this study are compared with the experimental data in literature (Sulaiman et al., 2015).

4. Results and discussion

It is reported in literature that the surface tension of NPs dispersed in deionized water increases with increasing concentration of NPs (Bhuiyan et al., 2015; Tanvir and Qiao, 2012; Vafaei et al., 2009; Moosavi et al., 2010). Figs. 1–3 show the validation of the results obtained from the proposed model in this study for NPs in deionized water using Li and Lu's equation for single electrolyte solution along with the Debye-Hückel constants to calculate the activities of the ions of NPs. The change in surface tension obtained from the proposed model ranges from 0.1 to 5 mN/m for concentration of NPs in deionized water between 0 and 5 wt%. The size of the NPs affects the surface tension for NPs dispersed in deionized water. The results obtained from the poropsed model for the effect of NPs size on the surface tension is in agreement with the ones reported by Bhuiyan et al. (2015). The results from this work reveal that the change in surface tension of NPs dispersed in deionized water will remain constant when the size of NPs is larger than 100 nm. Type curves for the change in surface tension of various NPs (including silica, alumina, and TiO_2) dispersed in deionized water against the concentration of NPs at different sizes of NPs are plotted under the assumption that the NPs are in contact with each other (as shown in Figs. 6–8).

The surface tension is negligible for size of NPs smaller than 0.1 nm as it is clear from Figs. 6–8. As the size of the NPs increases, the change in surface tension of the dispersed NPs in deionized water finds a logarithmic growth relationship with the concentration of the NPs.

Increase in the surface tension of the NPs in deionized water can be attributed to an increase in the mean ionic activity of the chemical dissociation reaction of NPs. The chemical equation of the dissociation of NPs in water can range from simple to complicated reactions as shown in Eqs. (43)–(53). Most of the NPs show more than two different chemical dissociation reactions. A simple chemical dissociation is assumed to dominate the solution at room temperature (25–30 °C) for all solutions of the NPs. The mean ionic activity is directly proportional to the valence electron of the NPs in solution. It is noted that the surface area to volume ratio has an exponential decay relationship with the size of the NPs. Therefore, increasing the surface tension of NPs in solution by increasing the size of the NPs can be directly related to the reduction in the surface area to volume ratio of NPs.

However, the surface tension of NPs in brine reduces with increasing the concentration of NPs as shown in Figs. 4 and 5. This

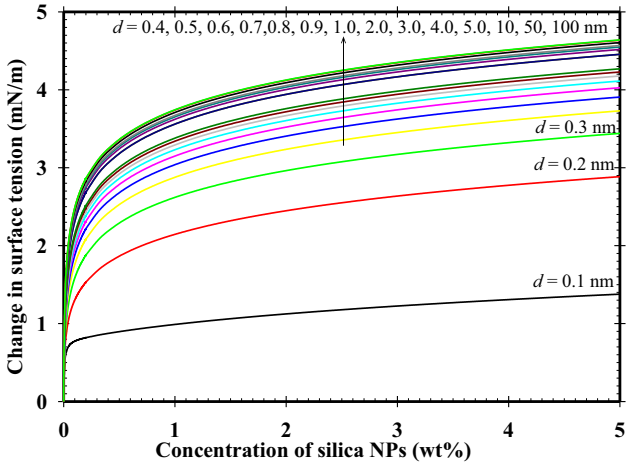

Fig. 6. Type curves for change in surface tension of dispersed silica NPs in deionized water versus concentration of silica NPs using the parameters listed in Tables 1 and 2.

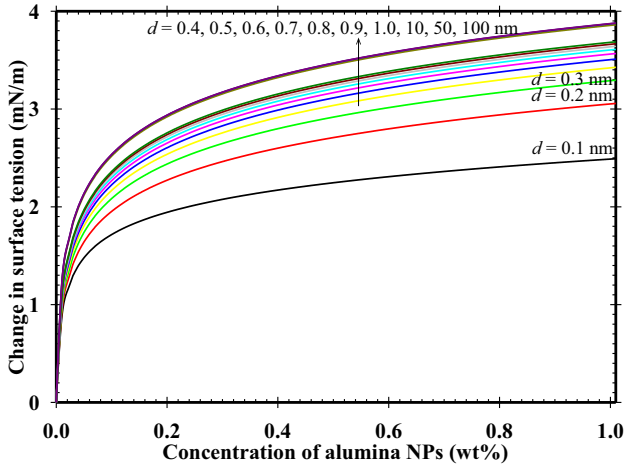

Fig. 7. Type curves for change in surface tension of dispersed alumina NPs in deionized water versus concentration of alumina NPs using the parameters listed in Tables 1 and 3.

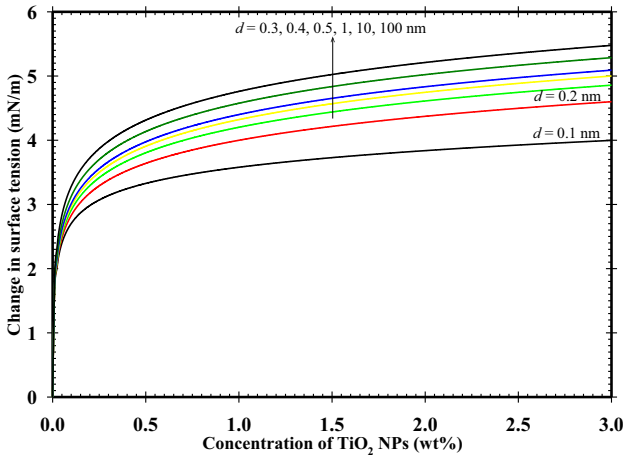

Fig. 8. Type curves for change in surface tension of dispersed TiO_2 NPs in deionized water versus concentration of TiO_2 NPs using the parameters listed in Tables 1 and 4.

behaviour of NPs in brine can be attributed to the dipole-dipole interaction and structural effects of the particles (Smith and Perkin, 2017). The presence of two decay lengths reported by Smith and Perkin (2017) for the addition of electrolyte into the polar liquid are due to the structural and monotonic screening (dipole-dipole) effects. The latter one is referred to electrostatic effect. Unlike the hard sphere particles that grow layer by layer, NPs create a discontinuous structure in the boundary with the unstructured form (Talapin et al., 2007; Wasan et al., 1992). The particles are spherical and arranged in the simple hexagonal form in the first layer along with the face-centred cubic (fcc) and the hexagonally closed packed (hcp) and the simple hexagonal form of packing in the second layer. The hexagonal structure can be attributed to the strong Coulombic interactions, the charge-dipole, the dipole-dipole, and the dispersive (Van der Waals) interactions (Talapin et al., 2007; Shim and Guyot-Sionnest, 1999). The presence of electrolytes in the dispersed solution of NPs creates the dipole-dipole interaction (Talapin et al., 2007).

The proposed model in this study excludes the Coulomb interaction because the NPs do not have neutral charges when they are dispersed in electrolyte solutions. The Van der Waals interaction of the molecules is also excluded because the aggregation of the particles should be avoided during the experimental determination of the surface tension. The dipole-dipole interaction of the particles will occur when the distance between the interacting particle dipoles exceeds the dimension of dipoles (Talapin et al., 2007). Fan and Striolo (2012) explained that the repulsive interaction of particles occurs when the distance between two NPs is 4.5 times the radius of the particle volume fraction. Therefore, the proposed model in this study used the assumption of constant volume fraction of the NPs at a constant concentration of the NaCl.

The size of the particles affects the type of structure (simple hexagonal, fcc, and hcp) and the orientation of the dipole moment (Drelich, 2016; Talapin et al., 2007). The proposed model in this study assumes that the dipole moment of the NPs and electrolyte ions are oriented parallel to each other along the x-y plane. The size of NPs in solution affects the electrolyte solution potential by compressing the electric double layer (Zhang et al., 2008). The centre to centre distance of the particles used for the dipole moment is in the range of 0–100 nm. Drelich (2016) explained that the centre to centre distance varies with the change in the size of the particles, while the electric double layer varies with variation in the particle volume fraction. In this study, it is assumed that the centre to centre distance of the NPs and the electrolyte ions and also the volume fraction of the NPs are constant.

Fig. 4 shows the validation of the results obtained from the proposed model in this study by the experimantal data reported by Zallaghi et al. (2018). The surface tension of NPs in brine reduces with increasing the concentration of NPs. However, the proposed model in this study slightly deviates from the reported experimental data at high concentrations. In this study, it is assumed that the dipole-dipole interaction and the structural effects are constant for all the concentrations of NPs. It is noted that the variation of the structural effect and dipole-dipole interaction with a change in the concentration of NPs is neglected. In addition, the Van der Waals force of interaction, which becomes significant with increasing the concentration of the NPs and the electrolyte in solutions as shown in Fig. 5, is neglected because the aggregation of the NPs should be avoided. The solutions of NPs should be stable and clear before they can be applied to the reservoirs in order to prevent plugging of the pore throats, which can reduce the rock permeability. Zallaghi et al. (2018) reported that the aggregation of silica NPs occurs at concentrations of NaCl larger than 30,000 ppm (3 wt%). The experimental data reported by Sulaiman et al. (2015) showed the surface tension becomes flat at 0.06 wt% concentration of the silica NPs and concentrations of NaCl larger than 2 wt%. This behaviour can be described by the increase in the effects of Van der Waals interaction and electrostatic repulsion. The dipole-dipole interaction reduces as the distance between the particles decreases with an increase in concentration. The deviation from the balance between the NPs and elctrolyte ions can lead to aggregation or dissolution, which occur at a critical salt concentration (CSC) defined by Khilar and Fogler (1984). Nikolov and Wasan (1989) explained that the addition of electrolyte to solutions of NPs reduces the electric double layer effect because the Debye inverse length increases. The volume fraction of the particles and the dipole-dipole effect decrease as the concentration of ecletrolytes increases. Therefore, the deviation of the obtained results in this study from the reported experimental data can be attributed to the assumption of constant structural effect and constant dipole-dipole interaction. The results obtained from the proposed model are in good agreement with the experimental data.

The application of the NPs at the field scale for EOR depends on the accurate prediction of the performance of the reservoir simulator. Currently, the available reservoir simulation software lacks the appropriate model to successfully determine the surface tension of NPs in the reservoir. Including the proposed model in the current reservoir simulators can improve the accuracy of history matching and prediction of recovery.

5. Conclusions

This study proposed a theoretical model to determine the change in surface tension of NPs in deionized waterby using the equation proposed by Li and Lu (2001) for single electrolyte solution combined with the Debye-Hückel constants to calculate the activities of the ions of NPs. The results obtained from the proposed model are in good agreement with the reported experimental data in literature. The proposed model can determine the change in surface tension of NPs in deionized water for different sizes of NPs.

This work includes the structural effect of NPs and the dipole-dipole interaction to propose a model that can determine the surface tension of NPs in brine. The model in this study extended the equation proposed by Borwankar and Wasan (1988) for surface excess adsorption of surfactants by combining the structural effect of particles and the dipole-dipole interaction to describe the excess surface adsorption of NPs in brine. The equation presented by Li and Lu (2001) for the surface tension of mixed electrolyte solution is extended to the NPs dispersed in brine by using the surface excess adsorption proposed in this study. The results obtained from the developed model are in good agreement with the

reported experimental data in literature. The deviation of the obtained results from the reported experimental data at high concnetrations of NPs and electrolytes can be attributed to the effect of Van der Waals interaction. The proposed model, which is used to determine the surface tension of both NPs in deionized water and NPs in brine, can assist the current simulators for accurate prediction of the reservoir perfomance.

Declaration of interest statement

There are no conflicts of interest to declare.

Acknowledgment

The financial support from the Department of Petroleum Engineering in the College of Engineering and Applied Science at the University of Wyoming is gratefully appreciated.

Appendix A. The effect of structural force on the chemical potential

The chemical potential of NPs in electrolyte solutions is affected by the diffuse layer, dipole-dipole interaction, and structural force. However, these forces are acting independently in the solution. The total chemical potential for a solution can be written as follows:

$$\mu_T = \mu_i + RT\ln c_i + zf_i\psi + pE + W^{os}(h) \tag{A1}$$

The solution is divided into two phases, which are the interface and the bulk phase. Therefore, Eq. (A1) can be written for the chemical potential of the interface as:

$$\mu_T^s = \mu_i^s + RT\ln c_i^s + zf_i\psi^s + pE + W^{os}(h) \tag{A2}$$

Using Eq. (1), the chemical potential of the bulk phase can be expressed as:

$$\mu_T^B = \mu_i^B + RT\ln c_i^B + zf_i\psi^B + pE + W^{os}(h) \tag{A3}$$

The effects of the diffuse layer, the dipole-dipole interaction, and the structural force are mainly taken into consideration in the double layer of the interface. These forces act independently and have no effect on the bulk phase. Therefore, the chemical potential of the bulk phase in Eq. (A3) can be written as follows:

$$\mu_T^B = \mu_i^B + RT\ln c_i^B \tag{A4}$$

It is considered that the solution is nonaqueous. Consequently, the chemical potential of the solution is due the structural force of the particles. This reduces the chemical potential of the interface, Eq. (A2), to:

$$\mu_T^s = \mu_i^s + RT\ln c_i^s + W^{os}(h) \tag{A5}$$

Since the chemical potential of an ion at the interface or diffuse layer is equal to that of the ion in the bulk phase and the standard potentials of the interface and the bulk phase are the same, the concentration of the interface can be expressed in tersm of the bulk concentration by equating Eqs. (A4) and (A5):

$$c_i^s = c_i^B \exp(-W^{os}(h)/kT)) \tag{A6}$$

For the structural force, the particle number density is expressed by Eq. (40). The particle density, which is the product of the particle number density, Eq. (40), and the amount of particles, can be expressed as:

$$\rho_{ci} = \frac{6\varphi}{\pi d^3} N \tag{A7}$$

where N is the amount of particles present in one unit volume of the solution and it is expressed as follows:

$$N = \frac{4}{3}\pi r^3 c(\infty) \tag{A8}$$

where r is the radius of the particle.

Therefore, the total density of the particles due to the structural force can be expressed as:

$$\rho_T = \sum_i \rho_{ci} c_i^s = \sum_i \rho_{ci} c(\infty) \exp\left(-\frac{W^{os}(h)}{kT}\right) \tag{A9}$$

The Poisson-Boltzmann equation for the diffuse layer due to the structural force can be expressed as follows:

$$\frac{d^2F}{dx^2} = -\frac{\sum_i \rho_{ci} c(\infty) \exp\left(-\frac{W^{os}(h)}{kT}\right)}{\varepsilon_0 \varepsilon_s} \tag{A10}$$

Using the differential equation with respect to the film thickness, h, for the ion of NPs, the field due to the structural force can be expressed as follows:

$$\frac{dF}{dh} = \sqrt{\frac{8kT\rho_{ci}c(\infty)}{\varepsilon_0\varepsilon_s}} \sinh\left(-\frac{W^{os}(h)}{2kT}\right) \tag{A11}$$

This expression, Eq. (A11), can result in the field due to the electrical double layer if the $F(h)$ is replaced by the potential energy and the ρ_{ci} is replaced by the charge density of the ions.

Substituting the field due to the structural force, Eq. (A11), into the ionic excess expression, Eq. (41), results in the following equation (which is used to obtain Eq. (42)):

$$\lambda_{SF} = c(\infty)\sqrt{\frac{\varepsilon_0\varepsilon_s}{8kT\rho_{ci}c(\infty)}} \int_{W^{os}(h)}^{\infty} \left(\frac{\exp(-W^{os}(h)/kT) - 1}{\sinh\left(-\frac{W^{os}(h)}{2kT}\right)}\right) dh \tag{A12}$$

Appendix B. The oscillatory period and the decay length of the particles

The oscillatory period and the decay length of the particles under oscillatory force in Eq. (38) are expressed, respectively, as follows (Kralchevsky and Denkov, 1995):

$$\frac{d_1}{d} = \sqrt{\frac{2}{3}} + a_1\Delta\varphi + a_2(\Delta\varphi)^2 \tag{B1}$$

$$\frac{d_2}{d} = \frac{b_1}{\Delta\varphi} - b_2 \qquad \text{where } \Delta\varphi \equiv \frac{\pi}{3\sqrt{2}} - \varphi \tag{B2}$$

The values of a_1, a_2, b_1, and b_2, which are defined as the slope and the intercept of the plots of the oscillatory period and the decay length versus the particle volume fraction, are 0.23728, 0.63300, 0.48663, and 0.42032, respectively (Kralchevsky and Denkov, 1995).

References

Adamson, A., Gast, A., 1997. Physical Chemical of Surfaces. Wiley, New York.
Alexander, G.B., Heston, W., Iler, R.K., 1954. The solubility of amorphous silica in water. J. Phys. Chem. 58 (6), 453–455.
Andreev, M., de Pablo, J.J., Chremos, A., Douglas, J.F., 2018. Influence of ion solvation on the properties of electrolyte solutions. J. Phys. Chem. B 122 (14), 4029–4034.
Ariyama, K., 1937. A theory of surface tension of aqueous solutions of inorganic acids. Bull. Chem. Soc. Jpn. 12 (3), 109–113.
Bassett, R.L., 1973. A Geochemical Investigation of Silica and Fluoride in the Unsaturated Zone of a Semi-Arid Environment. Texas Tech University.
Bera, A., Belhaj, H., 2016. Application of nanotechnology by means of nanoparticles and nanodispersions in oil recovery-A comprehensive review. J. Nat. Gas Sci. Eng. 34, 1284–1309.
Bhuiyan, M., Saidur, R., Amalina, M., Mostafizur, R., Islam, A., 2015. Effect of nanoparticles concentration and their sizes on surface tension of nanofluids. Procedia Eng. 105, 431–437.
Bolhuis, P.G., Frenkel, D., Mau, S.-C., Huse, D.A., 1997. Entropy difference between crystal phases. Nature 388 (6639), 235.

Borwankar, R., Wasan, D., 1988. Equilibrium, and dynamics of adsorption of surfactants at fluid-fluid interfaces. Chem. Eng. Sci. 43 (6), 1323–1337.

Buff, F.P., Stillinger Jr, F.H., 1956. Surface tension of ionic solutions. J. Chem. Phys. 25 (2), 312–318.

Chapman, D.L., 1913. LI A contribution to the theory of electrocapillarity. The London, Edinburgh, Dublin Philos. Mag. J. Sci. 25, 475–481.

Chen, H., Li, Z., Wang, F., Wang, Z., Zhihan, G., 2017. Extrapolation of surface tensions of electrolyte and associating mixtures solutions. Chem. Eng. Sci. 162, 10–20.

Cheng, H.-P., Barnett, R.N., Landman, U., 2002. Structure, collective hydrogen transfer, and formation of Si (OH) 4 in SiO 2–(H 2 O) n clusters. J. Chem. Phys. 116 (21), 9300–9304.

Cho, K.-S., Talapin, D.V., Gaschler, W., Murray, C.B., 2005. Designing PbSe nanowires and nanorings through oriented attachment of nanoparticles. J. Am. Chem. Soc. 127 (19), 7140–7147.

Christoffersen, J., Rostrup, E., Christoffersen, M.R., 1991. Relation between interfacial surface tension of electrolyte crystals in aqueous suspension and their solubility; a simple derivation based on surface nucleation. J. Cryst. Growth 113 (3–4), 599–605.

Debye, P., Hückel, E., 1923. De la theorie des electrolytes. I. abaissement du point de congelation et phenomenes associes. Physikalische Zeitschrift 24 (9), 185–206.

Drelich, J., 2016. Nanoparticles in a liquid: New state of liquid? J. Nanomater. Mol. Nanotechnol. 2013.

Drzymala, J., Lyklema, J., 2012. Surface tension of aqueous electrolyte solutions. Thermodynamics. J. Phys. Chem. A 116 (25), 6465–6472.

Engeset, B., 2012. The potential of hydrophilic silica nanoparticles for EOR purposes: A literature review and an experimental study Master Thesis. Department of Petroleum Engineering and Applied Geophysics, Norwegian University of Science and Technology, Trondheim, Norway.

Fan, H., Striolo, A., 2012. Nanoparticle effects on the water-oil interfacial tension. Phys. Rev. E 86 (5), 051610.

Fawcett, W.R., 2004. Liquids, Solutions, and, Interfaces: from Classical Macroscopic Descriptions to Modern Microscopic Details. Oxford University Press.

Ferdous, S., Ioannidis, M.A., Henneke, D.E., 2012. Effects of temperature, pH, and ionic strength on the adsorption of nanoparticles at liquid–liquid interfaces. J. Nanopart. Res. 14 (5), 850.

Fowkes, F.M., 1964. Attractive forces at interfaces. Ind. Eng. Chem. 56 (12), 40–52.

Fowkes, F.M., 1968. Calculation of work of adhesion by pair potential summation. J. Colloid Interface Sci. 28 (3–4), 493–505.

Franke, M.D., Ernst, W., Myerson, A., 1987. Kinetics of dissolution of alumina in acidic solution. AIChE J. 33 (2), 267–273.

Gibbs, J.W., 1906. The Scientific Papers of J. Willard Gibbs. Green and Company, Longmans.

Gouy, M., 1910. Sur la constitution de la charge électrique à la surface d'un électrolyte. J. Phys. Theor. Appl. 9 (1), 457–468.

Hachisu, S., Kobayashi, Y., Kose, A., 1973. Phase separation in monodisperse latexes. J. Colloid Interface Sci. 42 (2), 342–348.

Harikrishnan, A., Dhar, P., Agnihotri, P.K., Gedupudi, S., Das, S.K., 2017. Effects of interplay of nanoparticles, surfactants and base fluid on the surface tension of nanocolloids. Eur. Phys. J. E 40 (5), 53.

Hey, M.J., Shield, D.W., Speight, J.M., Will, M.C., 1981. Surface tensions of aqueous solutions of some 1: 1 electrolytes. J. Chem. Soc., Faraday Trans. 1: Phys. Chem. Condensed Phases 77 (1), 123–128.

Horn, R.G., Israelachvili, J., 1980. Direct measurement of forces due to solvent structure. Chem. Phys. Lett. 71 (2), 192–194.

Horvath, A.L., 1985. Handbook of Aqueous Electrolyte Solutions. Halsted Press.

James, R.O., Parks, G.A., 1982. Characterization of aqueous colloids by their electrical double-layer and intrinsic surface chemical properties. In: Surface and colloid science. Springer, pp. 119–216.

Jarvis, N.L., Scheiman, M.A., 1968. Surface potentials of aqueous electrolyte solutions. J. Phys. Chem. 72 (1), 74–78.

Jiang, L., Liu, Y., Zeng, G., Liu, S., Que, W., Li, J., Li, M., Wen, J., 2018. Adsorption of 17β-estradiol by graphene oxide: Effect of heteroaggregation with inorganic nanoparticles. Chem. Eng. J. 343, 371–378.

Kamal, M.S., Adewunmi, A.A., Sultan, A.S., Al-Hamad, M.F., Mehmood, U., 2017. Recent advances in nanoparticles enhanced oil recovery: rheology, interfacial tension, oil recovery, and wettability alteration. J. Nanomater. 2017.

Khilar, K.C., Fogler, H.S., 1984. The existence of a critical salt concentration for particle release. J. Colloid Interface Sci. 101 (1), 214–224.

Kobayashi, M., Petrykin, V.V., Kakihana, M., Tomita, K., Yoshimura, M., 2007. One-step synthesis of TiO2 (B) nanoparticles from a water-soluble titanium complex. Chem. Mater. 19 (22), 5373–5376.

Kralchevsky, P.A., Denkov, N.D., 1995. Analytical expression for the oscillatory structural surface force. Chem. Phys. Lett. 240 (4), 385–392.

Kruyt, H., 1952. General introduction. Colloid Sci. 1, 1–57.

Langmuir, I., 1918. The adsorption of gases on plane surfaces of glass, mica and platinum. J. Am. Chem. Soc. 40 (9), 1361–1403.

Laysandra, L., Sari, M.W.M.K., Soetaredjo, F.E., Foe, K., Putro, J.N., Kurniawan, A., Ju, Y.-H., Ismadji, S., 2017. Adsorption and photocatalytic performance of bentonite-titanium dioxide composites for methylene blue and rhodamine B decoloration. Heliyon 3 (12), e00488.

Lefevre, G., Duc, M., Lepeut, P., Caplain, R., Fédoroff, M., 2002. Hydration of γ-alumina in water and its effects on surface reactivity. Langmuir 18 (20), 7530–7537.

Li, Z.-B., Li, Y.-G., Lu, J.-F., 1999. Surface tension model for concentrated electrolyte aqueous solutions by the Pitzer equation. Ind. Eng. Chem. Res. 38 (3), 1133–1139.

Li, Z., Lu, B.C.-Y., 2001. Surface tension of aqueous electrolyte solutions at high concentrations—representation and prediction. Chem. Eng. Sci. 56 (8), 2879–2888.

Lorenz, P.B., 1950. The specific adsorption isotherms of thiocyanate and hydrogen ions at the free surface of aqueous solutions. J. Phys. Chem. 54 (5), 685–690.

Lucassen-Reynders, E., 1976. Adsorption of surfactant monolayers at gas/liquid and liquid/liquid interfaces. In: Progress in Surface and Membrane Science. Elsevier, pp. 253–360.

Markovich, T., Andelman, D., Podgornik, R., 2015. Surface tension of electrolyte interfaces: Ionic specificity within a field-theory approach. J. Chem. Phys. 142 (4), 044702.

McCabe, C., Galindo, A., 2010. SAFT Associating Fluids and Fluid Mixtures. Royal Society of Chemistry, London.

Metin, C.O., Baran, J.R., Nguyen, Q.P., 2012. Adsorption of surface functionalized silica nanoparticles onto mineral surfaces and decane/water interface. J. Nanopart. Res. 14 (11), 1246.

Moosavi, M., Goharshadi, E.K., Youssefi, A., 2010. Fabrication, characterization, and measurement of some physicochemical properties of ZnO nanofluids. Int. J. Heat Fluid Flow 31 (4), 599–605.

Müller, H.S., Woon, D.E., 2013. Calculated dipole moments for silicon and phosphorus compounds of astrophysical interest. J. Phys. Chem. A 117 (50), 13868–13877.

Negin, C., Ali, S., Xie, Q., 2016. Application of nanotechnology for enhancing oil recovery–a review. Petroleum 2 (4), 324–333.

Newton, R.C., Manning, C.E., 2003. Activity coefficient and polymerization of aqueous silica at 800 C, 12 kbar, from solubility measurements on SiO 2-buffering mineral assemblages. Contrib. Miner. Petrol. 146 (2), 135–143.

Nikolov, A., Wasan, D., 1989. Ordered micelle structuring in thin films formed from anionic surfactant solutions: I. Experimental. J. Colloid Interface Sci. 133 (1), 1–12.

Nikolov, A., Kralchevsky, P., Ivanov, I., Wasan, D., 1989. Ordered micelle structuring in thin films formed from anionic surfactant solutions: II. Model development. J. Colloid Interface Sci. 133 (1), 13–22.

Nikolov, A., Wasan, D., Denkov, N., Kralchevsky, P., Ivanov, I., 1990. Drainage of foam films in the presence of nonionic micelles. In: Surfactants and Macromolecules: Self-Assembly at Interfaces and in Bulk. Springer, pp. 87–98.

Nowotny, J., Norby, T., Bak, T., 2010. Reactivity between titanium dioxide and water at elevated temperatures. J. Phys. Chem. C 114 (42), 18215–18221.

O'Connor, T., Greenberg, S., 1958. The kinetics for the solution of silica in aqueous solutions. J. Phys. Chem. 62 (10), 1195–1198.

Olayiwola, S.O., Dejam, M., 2019. A comprehensive review on interaction of nanoparticles with low salinity water and surfactant for enhanced oil recovery in sandstone and carbonate reservoirs. Fuel 241, 1045–1057.

Onsager, L., Samaras, N.N., 1934. The surface tension of Debye-Hückel electrolytes. J. Chem. Phys. 2 (8), 528–536.

Petersen, P.B., Saykally, R.J., 2006. On the nature of ions at the liquid water surface. Annu. Rev. Phys. Chem. 57, 333–364.

Randles, J., 1977. Structure at the free surface of water and aqueous electrolyte solutions. Phys. Chem. Liq. 7 (1–2), 107–179.

Rimstidt, J.D., Barnes, H., 1980. The kinetics of silica-water reactions. Geochim. Cosmochim. Acta 44 (11), 1683–1699.

Shevchenko, E.V., Talapin, D.V., Kotov, N.A., O'brien, S., Murray, C.B., 2006. Structural diversity in binary nanoparticle superlattices. Nature 439 (7072), 55.

Shim, M., Guyot-Sionnest, P., 1999. Permanent dipole moment and charges in colloidal semiconductor quantum dots. J. Chem. Phys. 111 (15), 6955–6964.

Siracusa, P.A., Somasundaran, P., 1987. The role of mineral dissolution in the adsorption of dodecylbenzenesulfonate on kaolinite and alumina. Colloids Surf. 26, 55–77.

Smith, A.M., Perkin, S., 2017. Switching the structural force in ionic liquid-solvent mixtures by varying composition. Phys. Rev. Lett. 118 (9), 096002.

Stairs, R.A., 1995. Calculation of surface tension of salt solutions: effective polarizability of solvated ions. Can. J. Chem. 73 (6), 781–787.

Stillings, L.L., Brantley, S.L., 1995. Feldspar dissolution at 25 C and pH 3: Reaction stoichiometry and the effect of cations. Geochim. Cosmochim. Acta 59 (8), 1483–1496.

Sulaiman, W.R.W., Adala, A., Junin, R., Ismail, I., Ismail, A.R., Hamid, M.A., Kamaruddin, M.J., Zakaria, Z.Y., Johari, A., Hassim, M.H., 2015. Effects of Salinity on Nanosilica Applications in Altering Limestone Rock Wettability for Enhanced Oil Recovery. Advanced Materials Research. Trans Tech Publ.

Talapin, D.V., Shevchenko, E.V., Murray, C.B., Titov, A.V., Král, P., 2007. Dipole–dipole interactions in nanoparticle superlattices. Nano Lett. 7 (5), 1213–1219.

Tang, Z., Kotov, N.A., Giersig, M., 2002. Spontaneous organization of single CdTe nanoparticles into luminescent nanowires. Science 297 (5579), 237–240.

Tang, Z., Wang, Y., Podsiadlo, P., Kotov, N.A., 2006. Biomedical applications of layer-by-layer assembly: from biomimetics to tissue engineering. Adv. Mater. 18 (24), 3203–3224.

Tanvir, S., Qiao, L., 2012. Surface tension of nanofluid-type fuels containing suspended nanomaterials. Nanoscale Res. Lett. 7 (1), 226.

Vafaei, S., Purkayastha, A., Jain, A., Ramanath, G., Borca-Tasciuc, T., 2009. The effect of nanoparticles on the liquid–gas surface tension of Bi2Te3 nanofluids. Nanotechnology 20 (18). 185702.

Van Megen, W., Snook, I., 1976. Statistical mechanical approaches to phase transitions in hydrophobic colloids. I. effects of electrolyte concentration. J. Colloid Interface Sci. 57 (1), 40–46.

Wasan, D., Nikolov, A., Kralchevsky, P., Ivanov, I., 1992. Universality in film stratification due to colloid crystal formation. Colloids Surf. 67, 139–145.

Wasan, D.T., Nikolov, A.D., 2003. Spreading of nanofluids on solids. Nature 423 (6936), 156.
Weissenborn, P.K., Pugh, R.J., 1996. Surface tension of aqueous solutions of electrolytes: relationship with ion hydration, oxygen solubility, and bubble coalescence. J. Colloid Interface Sci. 184 (2), 550–563.
Zallaghi, M., Kharrat, R., Hashemi, A., 2018. Improving the microscopic sweep efficiency of water flooding using silica nanoparticles. J. Pet. Explor. Prod. Technol. 8 (1), 259–269.
Zargartalebi, M., Barati, N., Kharrat, R., 2014. Influences of hydrophilic and hydrophobic silica nanoparticles on anionic surfactant properties: interfacial and adsorption behaviors. J. Petrol. Sci. Eng. 119, 36–43.
Zhang, Y., Chen, Y., Westerhoff, P., Hristovski, K., Crittenden, J.C., 2008. Stability of commercial metal oxide nanoparticles in water. Water Res. 42 (8–9), 2204–2212.